Applied Acoustics 71 (2010) 690–700

Contents lists available at ScienceDirect

Applied Acoustics

journal homepage: www.elsevier.com/locate/apacoust

Analysis of mutiple-shepers radiation and scattering problems by using a null-field integral equation approach

Jeng-Tzong Chen [a,b,*], Ying-Te Lee [a], Yi-Jhou Lin [a]

[a] Department of Harbor and River Engineering, National Taiwan Ocean University, Keelung 20224, Taiwan
[b] Department of Mechanical and Mechanical Engineering, National Taiwan Ocean University, Keelung 20224, Taiwan

ARTICLE INFO

Article history:
Received 6 November 2009
Received in revised form 2 February 2010
Accepted 8 February 2010
Available online 8 April 2010

Keywords:
Scattering
Radiation
Null-field integral equation
Degenerate kernel
Spherical harmonics
Semi-analytical method

ABSTRACT

A systematic approach using the null-field integral equation in conjunction with the degenerate kernel is employed to solve the multiple radiation and scattering problems. Our approach can avoid calculating the principal values of singular and hypersingular integrals. Although we use the idea of null-field integral equation, we can locate the point on the real boundary thanks to the degenerate kernel. The proposed approach is seen as one kind of semi-analytical methods, since the error is attributed from the truncation of spherical harmonics. Finally, the numerical examples including one and two spheres are given to verify the validity of proposed approach.

1. Introduction

It is well known that the boundary integral equation methods (BIEMs) have been used to solve radiation and scattering problems for many years. Theoretically and practically speaking, the importance of the integral equation in the solution for certain types of boundary value problems is universally recognized. One of the problems frequently addressed in BIEM/BEM is the problem of irregular frequencies in boundary integral formulations for exterior acoustics and water wave problems. These frequencies are not physically realizable but are due to the numerical method, which has non-uniqueness solutions at characteristic frequencies associated with the eigenfrequency of the interior problem. Burton and Miller approach [1] as well as CHIEF technique [2] have been employed to deal with these problems.

Regarding the irregular frequency, a large amount of papers on acoustics have been published. For example, numerical examples for non-uniform radiation and scattering problems by using the dual BEM were provided and the irregular frequencies were detected and suppressed [3]. The non-uniqueness solution of radiation and scattering problems are numerically manifested in a rank deficiency of the influence coefficient matrix in BEM [1]. In order to obtain the unique solution, several integral equation formulations that provide additional constraints to the original system of equations have been proposed. Burton and Miller [1] proposed an integral equation that was valid for all wave numbers by forming a linear combination of the singular integral equation and its normal derivative. However, the calculation for the hypersingular integration is required. To avoid the computation of hypersingularity, Schenck [2] used an alternative method, the CHIEF method, which employs the boundary integral equations by collocating the interior point as an auxiliary condition to make up deficient constraint condition. Many researchers [4–6] applied the CHIEF method to deal with the problem of fictitious frequencies. If the chosen point locates on the nodal line of the associated interior eigenproblem, then this method may fail. To overcome this difficulty, Seybert and Rengarajan [4] and Wu and Seybert [5] employed a CHIEF-block method using the weighted residual formulation for acoustic problems. On the contrary, only a few papers on water wave for the non-uniqueness problem can be found. Ohmatsu [7] presented a combined integral equation method (CIEM), which was similar to the CHIEF-block method for acoustics proposed by Wu and Seybert [5]. In the CIEM, two additional constraints for one interior point result in an overdetermined system to insure the removal of irregular frequencies. An enhanced CHIEF method was also proposed by Lee and Wu [6].

* Corresponding author. Address: Department of Harbor and River Engineering, National Taiwan Ocean University, Keelung 20224, Taiwan. Tel.: +886 2 24622192x6177; fax: +886 2 24632375.
E-mail address: jtchen@mail.ntou.edu.tw (J.-T. Chen).

0003-682X/$ - see front matter © 2010 Elsevier Ltd. All rights reserved.
doi:10.1016/j.apacoust.2010.02.004

The main concern of the CHIEF method is how many numbers of interior points are required and where the positions should be located.

Recently, the appearance of irregular frequency in the method of fundamental solutions was also theoretically proved and numerically implemented [8]. However, as far as the present authors are aware, only a few papers have been published to date reporting on the efficacy of these methods in radiation and scattering problems involving more than one vibrating body. By this way, Dokumaci and Sarigül [9] discussed the fictitious frequency of radiation problem of two spheres. They used the surface Helmholtz integral equation (SHIE) and the CHIEF method to examine the position of fictitious frequency. However, some irregular frequencies were not suppressed by using the CHIEF technique and further investigation was required in their paper. In our formulation, we are also concerned with the fictitious frequency especially for the multiple spheres of scatterers and radiators. We will employ the Burton and Miller approach to avoid the CHIEF risk since hypersingularity can be tackled easily.

For three-dimensional radiation and scattering problems, many researchers have paid attention to solve the problems by using various approaches. Waterman [10] presented the *T*-matrix formulation for acoustic scattering problem. Peterson and Ström [11] extended the *T*-matrix approach to solve the problem with arbitrary number of scatterers. Liang and Lo [12] used the wave function method or so-called eigenfunction expansion method to analyze the electromagnetic wave scattering with two spheres. The wave function was expanded by the multipole expansion (or called addition theorem) and a series-form solution was represented. Gaunaurd and Huang [13] also used the multipole expansion to solve the problem, more detailed discussions were made due to the use of asymptotic approximations. Rao and Raju [14] used the method of moment to formulate the problem. The method was based on the potential theory and can be seen as one kind of indirect methods.

In the recent years, Chen and his group used the null-field integral equation formulation in conjunction with degenerate kernels and Fourier series to deal with many engineering problems with circular boundaries, such as torsion bar [15], water wave [16], Stokes flow [17], plate vibrations [18] and piezoelectricity problems [19]. They claimed that their approach has high accuracy of exponential convergence and is one kind of semi-analytical approaches. However, their applications only focused on two-dimensional problems. A review article can be found in [20]. In this paper, we would like to extend this idea to three-dimensional problems.

In this paper, a systematic approach using the null-field integral equation method in conjunction with the degenerate kernels is employed to solve the radiation and scattering problems of multiple spheres. By using the null-field integral equation instead of the boundary integral equation, we can avoid calculating the principal values of singular and hypersingular integrals. To fully utilize the spherical geometry, the fundamental solutions and the boundary densities are expanded by using degenerate kernels and spherical harmonics, respectively. Although the concept of null-field integral equation is used, the collocation point can be exactly located on the real boundary after introducing the degenerate kernel. At the same time, the singular and hypersingular integrals are transformed to series sum free of calculation using the principal value sense. The proposed approach is seen as one kind of semi-analytical methods, since the error only stems from the truncation of spherical harmonics. Regarding the nonunique problem (fictitious frequency), the Burton and Miller method instead of the CHIEF approach is used to eliminate the irregular frequency. Finally, not only one-sphere but also two-spheres radiation and scattering problems are given to verify the validity of the proposed approach.

2. Problem statement and the present approach

2.1. Problem statement

The problem considered in this paper is the acoustic scattering and radiation problems with multiple spheres. The problem is governed by the Helmholtz equation as follows:

$$(\nabla^2 + k^2)u(x) = 0, \quad x \in D, \tag{1}$$

where $u(x)$ is the scalar velocity potential, ∇^2 is the Lapalacian operator, k and D denote the wave number and the domain of interest, respectively. The sketch of multiple spheres is shown in Fig. 1.

2.2. Dual boundary integral equation formulation—the conventional version

The dual boundary integral formulation for the domain point is shown below:

$$u(x) = \int_S T(s,x)u(s)\,dS(s) - \int_S U(s,x)t(s)\,dS(s), \quad x \in D, \tag{2}$$

$$t(x) = \int_S M(s,x)u(s)\,dS(s) - \int_S L(s,x)t(s)\,dS(s), \quad x \in D, \tag{3}$$

where x and s are the field and source points, respectively, "S" is the spherical surface, $t(s)$ is the normal derivative on the source point, and the kernel function $U(s,x)$ is the fundamental solution which satisfies

$$(\nabla^2 + k^2)U(s,x) = -\delta(x-s), \tag{4}$$

where δ is the Dirac-delta function. The other kernel functions can be obtained as

$$T(s,x) = \frac{\partial U(s,x)}{\partial n_s}, \tag{5}$$

$$L(s,x) = \frac{\partial U(s,x)}{\partial n_x}, \tag{6}$$

$$M(s,x) = \frac{\partial^2 U(s,x)}{\partial n_x \partial n_s}, \tag{7}$$

where n_x and n_s denote the outward normal vector at the field point and the source point, respectively. If the collocation point x is on the boundary, the dual boundary integral equations for the boundary point can be obtained as follows:

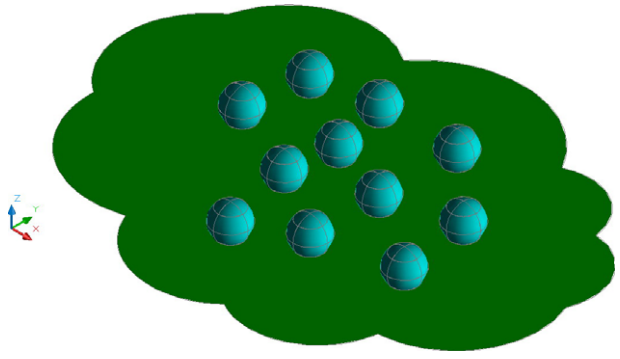

Fig. 1. Sketch of multiple spheres.

$$\frac{1}{2}u(x) = C.P.V.\int_S T(s,x)u(s)\,dS(s) - R.P.V.\int_S U(s,x)t(s)\,dS(s), \quad x \in B, \tag{8}$$

$$\frac{1}{2}t(x) = H.P.V.\int_S M(s,x)u(s)\,dS(s) - C.P.V.\int_S L(s,x)t(s)\,dS(s), \quad x \in B, \tag{9}$$

where *R.P.V*, *C.P.V* and *H.P.V* are the Riemann principal value, the Cauchy principal value and the Hadamard (or called Mangler) principal value, respectively. By collocating x outside the domain, we obtain the null-field integral equation as shown below:

$$0 = \int_S T(s,x)u(s)\,dS(s) - \int_S U(s,x)t(s)\,dS(s), \quad x \in D^c, \tag{10}$$

$$0 = \int_S M(s,x)u(s)\,dS(s) - \int_S L(s,x)t(s)\,dS(s), \quad x \in D^c, \tag{11}$$

where D^c denotes the complementary domain.

2.3. Dual null-field integral equation formulation—the present version

By introducing the degenerate kernels for the fundamental solution, the collocation points can be located on the real boundary free of facing singularity. Therefore, the representations of integral equations including the boundary point can be written as

$$u(x) = \int_S T^e(s,x)u(s)\,dS(s) - \int_S U^e(s,x)t(s)\,dS(s), \quad x \in D \cup S, \tag{12}$$

$$t(x) = \int_S M^e(s,x)u(s)\,dS(s) - \int_S L^e(s,x)t(s)\,dS(s), \quad x \in D \cup S, \tag{13}$$

and

$$0 = \int_S T^i(s,x)u(s)\,dS(s) - \int_S U^i(s,x)t(s)\,dS(s), \quad x \in D^c \cup S, \tag{14}$$

$$0 = \int_S M^i(s,x)u(s)\,dS(s) - \int_S L^i(s,x)t(s)\,dS(s), \quad x \in D^c \cup S, \tag{15}$$

once the interior "*i*" or exterior "*e*" kernel is expressed in terms of an appropriate degenerate form. It is found that the collocation point is categorized to three positions, domain (Eqs. (2) and (3)), boundary (Eqs. (8) and (9)) and complementary domain (Eqs. (10) and (11)) in the conventional formulation. After using the degenerate kernel for the null-field BIEM, both Eqs. (12) and (13) and Eqs. (14) and (15) can contain the boundary point.

2.4. Expansions of the fundamental solution and boundary density

The fundamental solution as previously mentioned in Eq. (4) is

$$U(s,x) = \frac{e^{-ikr}}{4\pi r}, \tag{16}$$

where $r \equiv |s-x|$ is the distance between the source point and the field point and i is the imaginary number with $i^2 = -1$. To fully utilize the property of spherical geometry, the mathematical tools, degenerate (separable or finite rank) kernel and spherical harmonics, are utilized for the analytical calculation of boundary integrals.

2.4.1. Degenerate (separable) kernel for fundamental solutions

In the spherical coordinate, the field point, x, and source point, s, can be expressed as $x = (\rho,\theta,\phi)$ and $s = (\bar\rho,\bar\theta,\bar\phi)$ in the spherical coordinates, respectively. By employing the addition theorem for separating the source point and field point, the kernel functions, $U(s,x)$, $T(s,x)$, $L(s,x)$ and $M(s,x)$, are expanded in terms of degenerate kernel as shown below:

$$U(s,x) = \begin{cases} U^i(\bar\rho,\bar\theta,\bar\phi;\rho,\theta,\phi) = \frac{ik}{4\pi}\sum_{n=0}^{\infty}(2n+1)\sum_{m=0}^{n}\varepsilon_m\frac{(n-m)!}{(n+m)!} \\ P_n^m(\cos\theta)P_n^m(\cos\bar\theta)j_n(k\rho)h_n^{(2)}(k\bar\rho)\cos[m(\bar\phi-\phi)], \\ \quad \bar\rho \geqslant \rho, \\ U^e(\bar\rho,\bar\theta,\bar\phi;\rho,\theta,\phi) = \frac{ik}{4\pi}\sum_{n=0}^{\infty}(2n+1)\sum_{m=0}^{n}\varepsilon_m\frac{(n-m)!}{(n+m)!} \\ P_n^m(\cos\theta)P_n^m(\cos\bar\theta)j_n(k\bar\rho)h_n^{(2)}(k\rho)\cos[m(\bar\phi-\phi)], \\ \quad \bar\rho < \rho, \end{cases} \tag{17}$$

$$T(s,x) = \begin{cases} T^i(\bar\rho,\bar\theta,\bar\phi;\rho,\theta,\phi) = \frac{ik^2}{4\pi}\sum_{n=0}^{\infty}(2n+1)\sum_{m=0}^{n}\varepsilon_m\frac{(n-m)!}{(n+m)!} \\ P_n^m(\cos\theta)P_n^m(\cos\bar\theta)j_n(k\rho)h_n^{\prime(2)}(k\bar\rho)\cos[m(\bar\phi-\phi)], \\ \quad \bar\rho > \rho, \\ T^e(\bar\rho,\bar\theta,\bar\phi;\rho,\theta,\phi) = \frac{ik}{4\pi}\sum_{n=0}^{\infty}(2n+1)\sum_{m=0}^{n}\varepsilon_m\frac{(n-m)!}{(n+m)!} \\ P_n^m(\cos\theta)P_n^m(\cos\bar\theta)j_n'(k\bar\rho)h_n^{(2)}(k\rho)\cos[m(\bar\phi-\phi)], \\ \quad \bar\rho < \rho, \end{cases} \tag{18}$$

$$L(s,x) = \begin{cases} L^i(\bar\rho,\bar\theta,\bar\phi;\rho,\theta,\phi) = \frac{ik^2}{4\pi}\sum_{n=0}^{\infty}(2n+1)\sum_{m=0}^{n}\varepsilon_m\frac{(n-m)!}{(n+m)!} \\ P_n^m(\cos\theta)P_n^m(\cos\bar\theta)j_n'(k\rho)h_n^{(2)}(k\bar\rho)\cos[m(\bar\phi-\phi)], \\ \quad \bar\rho > \rho, \\ L^e(\bar\rho,\bar\theta,\bar\phi;\rho,\theta,\phi) = \frac{ik^2}{4\pi}\sum_{n=0}^{\infty}(2n+1)\sum_{m=0}^{n}\varepsilon_m\frac{(n-m)!}{(n+m)!} \\ P_n^m(\cos\theta)P_n^m(\cos\bar\theta)j_n(k\bar\rho)h_n^{\prime(2)}(k\rho)\cos[m(\bar\phi-\phi)], \\ \quad \bar\rho < \rho, \end{cases} \tag{19}$$

$$M(s,x) = \begin{cases} M^i(\bar\rho,\bar\theta,\bar\phi;\rho,\theta,\phi) = \frac{ik^3}{4\pi}\sum_{n=0}^{\infty}(2n+1)\sum_{m=0}^{n}\varepsilon_m\frac{(n-m)!}{(n+m)!} \\ P_n^m(\cos\theta)P_n^m(\cos\bar\theta)j_n'(k\rho)h_n^{\prime(2)}(k\bar\rho)\cos[m(\bar\phi-\phi)], \\ \quad \bar\rho \geqslant \rho, \\ M^e(\bar\rho,\bar\theta,\bar\phi;\rho,\theta,\phi) = \frac{ik^3}{4\pi}\sum_{n=0}^{\infty}(2n+1)\sum_{m=0}^{n}\varepsilon_m\frac{(n-m)!}{(n+m)!} \\ P_n^m(\cos\theta)P_n^m(\cos\bar\theta)j_n'(k\bar\rho)h_n^{\prime(2)}(k\rho)\cos[m(\bar\phi-\phi)], \\ \quad \bar\rho < \rho, \end{cases} \tag{20}$$

where the superscripts "*i* " and "*e*" denote the interior and exterior regions, j_n and $h_n^{(2)}$ are the nth order spherical Bessel function of the first kind and the nth order spherical Hankel function of the second kind, respectively, P_n^m is the associated Lengendre polynomial and ε_m is the Neumann factor,

$$\varepsilon_m = \begin{cases} 1, & m = 0, \\ 2, & m = 1,2,\ldots,\infty. \end{cases} \tag{21}$$

It is noted that U and M kernels in Eqs. (17) and (20) contain the equal sign of $\rho = \bar\rho$ while T and L kernels do not include the equal sign due to discontinuity.

2.4.2. Spherical harmonics expansion for boundary densities

We apply the spherical harmonics expansion to approximate the boundary density and its normal derivative on the surface of sphere. Therefore, the following expressions can be obtained:

$$u_i(s) = \sum_{v=0}^{\infty}\sum_{w=0}^{v}A_{vw}^i P_v^w(\cos\bar\theta)\cos(w\bar\phi), \quad s \in B_i, \tag{22}$$

$$t_i(s) = \sum_{v=0}^{\infty}\sum_{w=0}^{v}B_{vw}^i P_v^w(\cos\bar\theta)\cos(w\bar\phi), \quad s \in B_i, \tag{23}$$

where A_{vw}^i and B_{vw}^i are the unknown spherical coefficients on $B_i (i = 1,2,\ldots)$. However, only M finite number of truncated terms for v is used in the real implementation.

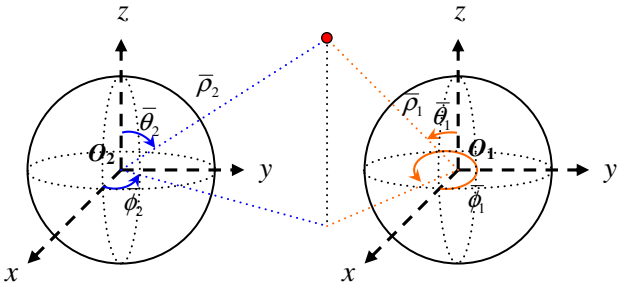

Fig. 2. Adaptive observer system.

2.5. Adaptive observer system

Since the boundary integral equations are frame indifferent, i.e. rule of objectivity is obeyed. Adaptive observer system is chosen to fully employ the property of degenerate kernels. Fig. 2 shows the boundary integration for the spherical boundaries. It is worthy of noting that the origin of the observer system can be adaptively located on the center of the corresponding circle under integration to fully utilize the geometry of sphere. The dummy variable in the integration on the surface are the angles ($\bar{\theta}$ and $\bar{\phi}$). By using the adaptive observer system, all the boundary integrals can be determined analytically through series sum instead of using the concept of principal values.

2.6. Linear algebraic equation

In order to calculate the $P(P=(M+2)(M+1)/2)$ unknown spherical harmonics, P boundary points on each spherical surface are needed to be collocated. By collocating the null-field point exactly on the kth spherical surface for Eqs. (14) and (15), we have

$$0=\sum_{j=1}^{N}\int_{S_j}T^i(s,x_k)u(s)\,dS(s)-\sum_{j=1}^{N}\int_{S_j}U^i(s,x_k)t(s)\,dS(s),\quad x_k\in D^c\cup S, \tag{24}$$

$$0=\sum_{j=1}^{N}\int_{S_j}M^i(s,x_k)u(s)\,dS(s)-\sum_{j=1}^{N}\int_{S_j}L^i(s,x_k)t(s)\,dS(s),\quad x_k\in D^c\cup S, \tag{25}$$

where N is the number of spheres. For the S_j boundary integral of the spherical surface, the kernels of $U(s,x)$, $T(s,x)$, $L(s,x)$ and $M(s,x)$ are respectively expressed in terms of degenerate kernels of Eqs. (17) and (20) with respect to the observer origin at the center of S_j . The boundary densities of $u(s)$ and $t(s)$ are substituted by using the spherical boundary harmonics of Eqs. (22) and (23), respectively. In the $dS(s)$ integration, we set the origin of the observer system to collocate at the center O_j of boundary S_j to fully utilize the degenerate kernel and spherical harmonics. By locating the null-field point on the real surface S_k from outside of the domain D^c in the numerical implementation, linear algebraic systems are obtained as

$$[\mathbf{U}]\{\mathbf{t}\}=[\mathbf{T}]\{\mathbf{u}\}, \tag{26}$$

$$[\mathbf{L}]\{\mathbf{t}\}=[\mathbf{M}]\{\mathbf{u}\}, \tag{27}$$

where [**U**], [**T**], [**L**] and [**M**] are the influence matrices with a dimension of $(N\times P)$ by $(N\times P)$, and {**t**} and {**u**} denote the vectors for $t(s)$ and $u(s)$ of the spherical harmonics coefficients with a dimension of $(N\times P)$ by 1, in which, [**U**], [**T**], [**L**], [**M**], {**u**} and {**t**} can be defined as follows:

$$[\mathbf{U}]=[\mathbf{U}_{\alpha\beta}]=\begin{bmatrix}\mathbf{U}_{11}&\mathbf{U}_{12}&\cdots&\mathbf{U}_{1N}\\ \mathbf{U}_{21}&\mathbf{U}_{22}&\cdots&\mathbf{U}_{2N}\\ \vdots&\vdots&\ddots&\vdots\\ \mathbf{U}_{N1}&\mathbf{U}_{N2}&\cdots&\mathbf{U}_{NN}\end{bmatrix}, \tag{28}$$

$$[\mathbf{T}]=[\mathbf{T}_{\alpha\beta}]=\begin{bmatrix}\mathbf{T}_{11}&\mathbf{T}_{12}&\cdots&\mathbf{T}_{1N}\\ \mathbf{T}_{21}&\mathbf{T}_{22}&\cdots&\mathbf{T}_{2N}\\ \vdots&\vdots&\ddots&\vdots\\ \mathbf{T}_{N1}&\mathbf{T}_{N2}&\cdots&\mathbf{T}_{NN}\end{bmatrix}, \tag{29}$$

$$[\mathbf{L}]=[\mathbf{L}_{\alpha\beta}]=\begin{bmatrix}\mathbf{L}_{11}&\mathbf{L}_{12}&\cdots&\mathbf{L}_{1N}\\ \mathbf{L}_{21}&\mathbf{L}_{22}&\cdots&\mathbf{L}_{2N}\\ \vdots&\vdots&\ddots&\vdots\\ \mathbf{L}_{N1}&\mathbf{L}_{N2}&\cdots&\mathbf{L}_{NN}\end{bmatrix}, \tag{30}$$

$$[\mathbf{M}]=[\mathbf{M}_{\alpha\beta}]=\begin{bmatrix}\mathbf{M}_{11}&\mathbf{M}_{12}&\cdots&\mathbf{M}_{1N}\\ \mathbf{M}_{21}&\mathbf{M}_{22}&\cdots&\mathbf{M}_{2N}\\ \vdots&\vdots&\ddots&\vdots\\ \mathbf{M}_{N1}&\mathbf{M}_{N2}&\cdots&\mathbf{M}_{NN}\end{bmatrix}, \tag{31}$$

$$\{\mathbf{u}\}=\begin{Bmatrix}\mathbf{u}_1\\ \mathbf{u}_2\\ \vdots\\ \mathbf{u}_N\end{Bmatrix},\quad \{\mathbf{t}\}=\begin{Bmatrix}\mathbf{t}_1\\ \mathbf{t}_2\\ \vdots\\ \mathbf{t}_N\end{Bmatrix}, \tag{32}$$

where the vectors $\{\mathbf{u}_k\}$ and $\{\mathbf{t}_k\}$ are in the form of $\left\{A_{00}^k\quad A_{10}^k\quad A_{11}^k\cdots A_{PP}^k\right\}^T$ and $\left\{B_{00}^k\quad B_{10}^k\quad B_{11}^k\quad\cdots\quad B_{PP}^k\right\}^T$; the first subscript "$\alpha$" $(\alpha=1,2,\ldots,N)$ in the $[\mathbf{U}_{\alpha\beta}]$ denotes the index of the αth sphere where the collocation point is located and the second subscript "β" $(\beta=1,2,\ldots,N)$ denotes the index of the βth sphere in which the boundary data $\{\mathbf{u}_k\}$ or $\{\mathbf{t}_k\}$ are specified. The coefficient matrix of the linear algebraic system is partitioned into blocks, and each diagonal block $(\mathbf{U}_{pp})$ corresponds to the influence matrices due to the same sphere of collocation and spherical harmonics expansion. After collocating the point along the αth spherical surface, the elements of $[\mathbf{U}_{\alpha\beta}]$, $[\mathbf{T}_{\alpha\beta}]$, $[\mathbf{L}_{\alpha\beta}]$ and $[\mathbf{M}_{\alpha\beta}]$ are defined as

$$U_{\alpha\beta}=\int_{S_k}\int U(s_k,x_m)\bar{\rho}^2\,d\bar{\phi}_k\,d\bar{\theta}_k, \tag{33}$$

$$T_{\alpha\beta}=\int_{S_k}\int T(s_k,x_m)\bar{\rho}^2\,d\bar{\phi}_k\,d\bar{\theta}_k, \tag{34}$$

$$L_{\alpha\beta}=\int_{S_k}\int L(s_k,x_m)\bar{\rho}^2\,d\bar{\phi}_k\,d\bar{\theta}_k, \tag{35}$$

$$M_{\alpha\beta}=\int_{S_k}\int M(s_k,x_m)\bar{\rho}^2\,d\bar{\phi}_k\,d\bar{\theta}_k, \tag{36}$$

where $\bar{\phi}_k$ and $\bar{\theta}_k(k=1,2,\ldots,N)$ are the spherical angles of the spherical coordinates. After obtaining the unknown spherical harmonics, interior potentials can be obtained by using Eq. (12).

2.7. Potential gradient

Since the fictitious frequencies exist in the radiation and scattering problems, some remedies are used to overcome the problems. Therefore, the *LM* formulation is to play an important role. The potential gradient on the boundary is required to calculate. For the multiple radiation or scattering, the field point and source point may not be located on the same spherical boundary. The normal derivative should be taken special care as the source and field points are located on different spherical boundaries. As shown in Fig. 3 where collocation point is located on the spherical boundary S_i and the integration path is on the spherical boundary S_j, the origin is set at the center of the jth sphere under integration. The true normal direction with respect to the collocation point x is $\hat{e}_1$. The

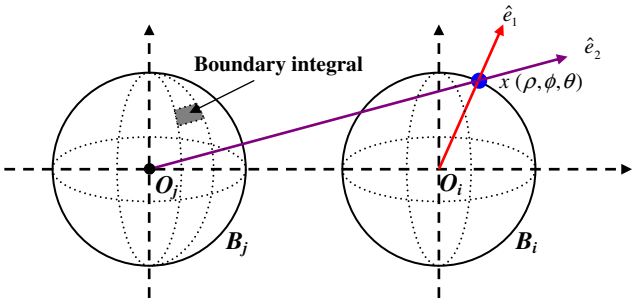

Fig. 3. Decomposition of potential gradient.

incorrect vector for the normal derivative, $\hat{e}_2$, is obtained when the L and M kernels are directly used. Therefore, it needs modification. According to the definition of normal derivative in the Cartesian coordinates, we obtain

$$t(x) = \frac{\partial u(x)}{\partial n_x} = \nabla u \cdot \mathbf{n}_x, \tag{37}$$

where

$$\nabla u = \frac{\partial u}{\partial x}\vec{i} + \frac{\partial u}{\partial y}\vec{j} + \frac{\partial u}{\partial z}\vec{k}. \tag{38}$$

Based on the chain rule, we have

$$\frac{\partial u}{\partial x} = \frac{\partial u}{\partial \rho}\frac{\partial \rho}{\partial x} + \frac{\partial u}{\partial \theta}\frac{\partial \theta}{\partial x} + \frac{\partial u}{\partial \phi}\frac{\partial \phi}{\partial x}, \tag{39}$$

$$\frac{\partial u}{\partial y} = \frac{\partial u}{\partial \rho}\frac{\partial \rho}{\partial y} + \frac{\partial u}{\partial \theta}\frac{\partial \theta}{\partial y} + \frac{\partial u}{\partial \phi}\frac{\partial \phi}{\partial y}, \tag{40}$$

$$\frac{\partial u}{\partial z} = \frac{\partial u}{\partial \rho}\frac{\partial \rho}{\partial z} + \frac{\partial u}{\partial \theta}\frac{\partial \theta}{\partial z} + \frac{\partial u}{\partial \phi}\frac{\partial \phi}{\partial z}. \tag{41}$$

Potential gradients can be expanded into

$$\frac{\partial u}{\partial x} = \sin\theta\cos\phi\frac{\partial u}{\partial \rho} + \frac{\cos\theta\cos\phi}{\rho}\frac{\partial u}{\partial \theta} - \frac{\sin\phi}{\rho\sin\theta}\frac{\partial u}{\partial \phi}, \tag{42}$$

$$\frac{\partial u}{\partial y} = \sin\theta\sin\phi\frac{\partial u}{\partial \rho} + \frac{\cos\theta\sin\phi}{\rho}\frac{\partial u}{\partial \theta} + \frac{\cos\phi}{\rho\sin\theta}\frac{\partial u}{\partial \phi}, \tag{43}$$

$$\frac{\partial u}{\partial z} = \cos\theta\frac{\partial u}{\partial \rho} - \frac{\sin\theta}{\rho}\frac{\partial u}{\partial \theta}. \tag{44}$$

According to Eq. (37), the right normal derivative of the potential can be obtained by considering $\mathbf{n}_x = \hat{e}_1$. The flowchart of the present method is shown in Fig. 4.

3. Numerical examples

Here, four cases including radiation and scattering problems for single and double spheres are given to demonstrate the validity of proposed approach. Case 1 is the one-sphere radiation problem subject to various boundary conditions. The analytical solution is derived and is compared with others. Two-spheres radiation problem is considered in Case 2. The numerical solution in [9] is given to compare with the solution of the present approach. Case 3 is a scattering problem of a single sphere subject to an incident wave. The final case of a two-spheres scattering problem solved by Peterson and Ström [11] is revisited to verify the validity of our approach. It is noted that the fundamental solution of the second kind spherical Hankel function is chosen for radiation problems (Cases 1 and 2) and the first kind spherical Hankel function for scattering problems (Cases 3 and 4) in order to compare with other results in the literature.

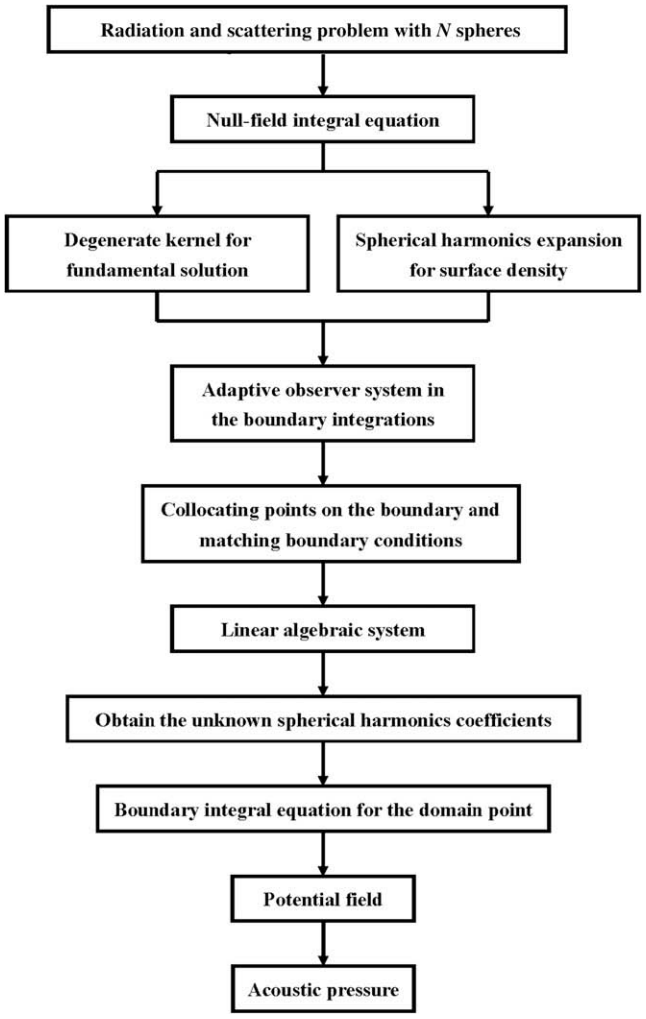

Fig. 4. Flowchart of the present method.

Case 1 A sphere pulsating with uniform radial velocity or oscillating with non-uniform radial velocity

In the first case, we concerned with the two situations of a sphere. One is the sphere pulsating with uniform radial velocity and another is the sphere oscillating with non-uniform radial velocity. When a sphere is pulsating with uniform radial velocity U_0, the exact solution of the problem can be found in [21] as shown below:

$$p(\rho) = \frac{a}{\rho}\left(\frac{iz_0ka}{1+ika}\right)U_0e^{-ik(\rho-a)}, \tag{45}$$

where z_0 is the characteristic impedance of the medium $z_0 = \rho_0 c$ in which ρ_0 is the density of the medium at rest and c is the sound velocity, and p is the sound pressure which is defined as

$$p(\rho) = -i\rho_0\omega u(\rho) = -iz_0ku(\rho), \tag{46}$$

in which ω is the angular frequency and k is the wave number that equals to the angular frequency over sound velocity. After expanding the surface density by using spherical harmonics, we have

$$B_{00} = U_0, \tag{47}$$

and the other coefficients are zero. Then, the unknown coefficient can be obtained as follows:

$$A_{00} = -\frac{1}{k}\frac{h_0^{(2)}(ka)}{h_0'^{(2)}(ka)}U_0, \tag{48}$$

by using Eq. (14). After obtaining the unknown coefficient, we have

$$p(\rho) = -iz_0U_0\frac{h_0^{(2)}(k\rho)}{h_0'^{(2)}(ka)}. \tag{49}$$

The expression of Eq. (49) seems to look different from the exact solution in Eq. (43). However, the spherical Hankel function can be represented by using the series form found in [22] as shown below:

$$h_0^{(2)}(z) = i^{n+1}z^{-1}e^{-iz}\sum_{m=0}^{n}\frac{(n+m)!}{m!\Gamma(n-m+1)}(-2iz)^{-m}. \tag{50}$$

After substituting Eq. (50) into Eq. (49), the result of our approach looks neater and yields the same exact solution of Eq. (45). For the numerical implementation, M is chosen to be 6 and 28 nodes are distributed on the spherical surface as shown in Fig. 5. Fig. 6a and b show the real and imaginary parts of non-dimensional pressure on the surface by using the numerical procedure. In Fig. 6a and b, irregular frequency does not appear due to the analytical cancellation of zero divided by zero in our formulation. However, Seybert et al. [21] needed to improve their result by using the CHIEF method. For this point, we can claim that our approach is more accurate than that of Seybert et al. [21].

In another situation for the oscillating surface with radial velocity, $U_0\cos\theta$, the exact solution is also found in [21] as

$$p(\rho,\theta) = \left(\frac{a}{\rho}\right)^2\left[\frac{iz_0ka(1+ik\rho)}{2(1+ika)-k^2a^2}\right](U_0\cos\theta)e^{-ik(\rho-a)}. \tag{51}$$

After expanding the boundary density by using the spherical harmonics, we have

$$B_{10} = U_0, \tag{52}$$

and the other coefficients are zero. Then, the unknown coefficient can be obtained as follows:

$$A_{10} = -\frac{1}{k}\frac{h_1^{(2)}(ka)}{h_1'^{(2)}(ka)}U_0, \tag{53}$$

by using Eq. (14). After obtaining the unknown coefficient, we have

$$p(\rho,\theta) = -iz_0U_0\frac{h_1^{(2)}(k\rho)}{h_2'^{(2)}(ka)}\cos\theta. \tag{54}$$

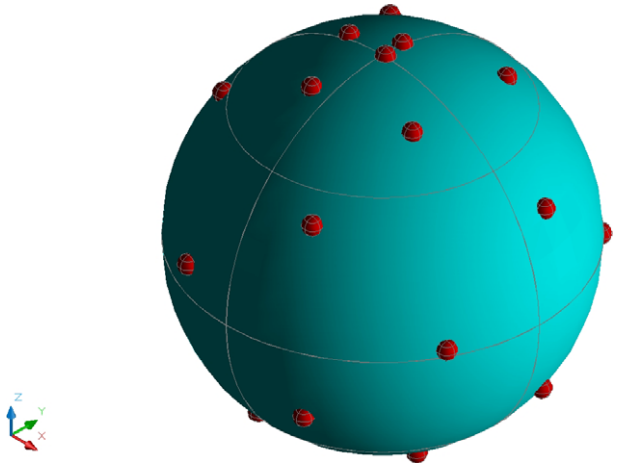

Fig. 5. Distribution of collocation points for a sphere ($M = 6$).

Similarly, the present solution of Eq. (54) seems to be not equivalent to the exact solution of Eq. (51) for the first glance. After substituting series form of the spherical Hankel function, we can prove the mathematical equivalence between Eqs. (54) and (51).

Case 2 Two-spheres vibrating from uniform radial velocity

After successfully solving one-sphere case, we extend our approach to deal with the two-spheres radiation problem [9]. As shown in Fig. 7, the two spheres vibrate with uniform radial velocity U_0. In the real calculation, we choose M to be 10. Sixty-six nodes are distributed on each sphere as shown in Fig. 8. Figs. 9–11a show the pressure contours of two dilating spherical sources at the hor-

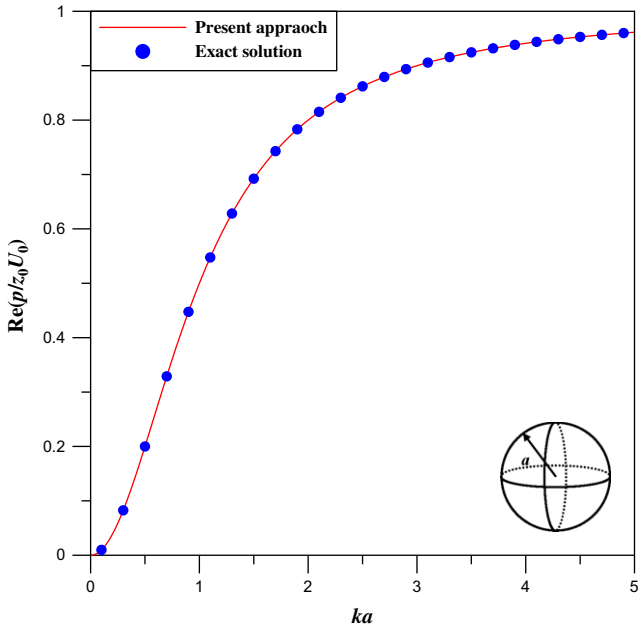

Fig. 6a. Real part of non-dimensional pressure on the surface.

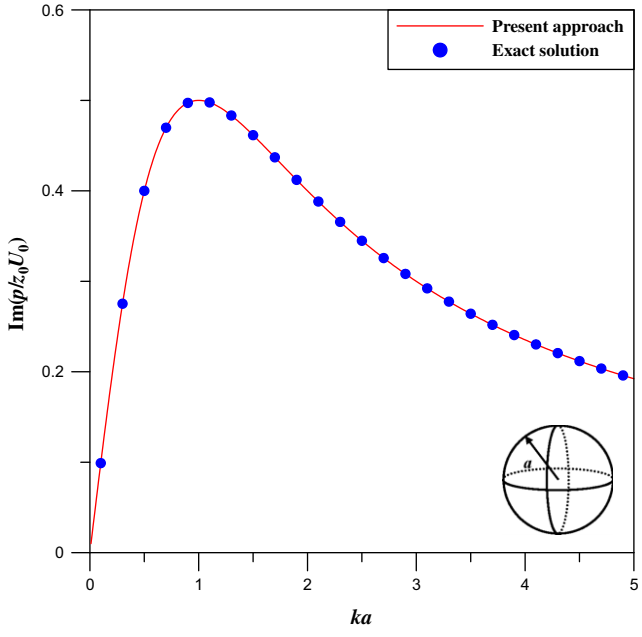

Fig. 6b. Imaginary part of non-dimensional pressure on the surface.

izontal plane of $z = 0$ for $ka = 1,2$ and 0.1, respectively, by using the SHIE [9]. Figs. 9–11b are the corresponding results by using the present approach. After comparing our results with those of SHIE [9], good agreement is observed. For the spherical geometry problem, the symmetry property results in high degeneracy. The number of degenerate eigenvalues at the characteristic frequency becomes large. Therefore, the risk of CHIEF point becomes possible. How to choose the location of CHIEF point and how many the CHIEF points are sufficient to overcome the irregular problem plays an important role. Therefore, we adopt the Burton and Miller method to remedy the irregular frequency. It is not free of worrying about the calculation of hypersingular integrals since the singular and hypersingular integrals are determined in an alternative way. Fig. 12a and b shows the potentials on the nearest point and furthest point, respectively. It is observed that the irregular frequencies are successfully suppressed.

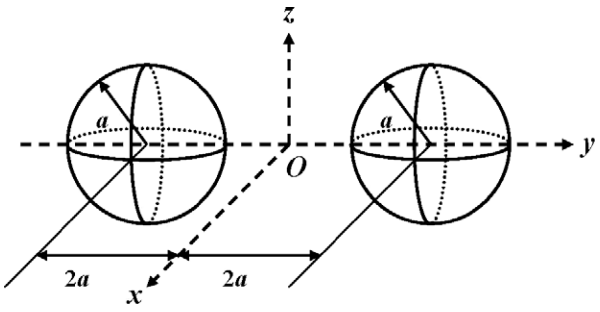

Fig. 7. Sketch of two spheres.

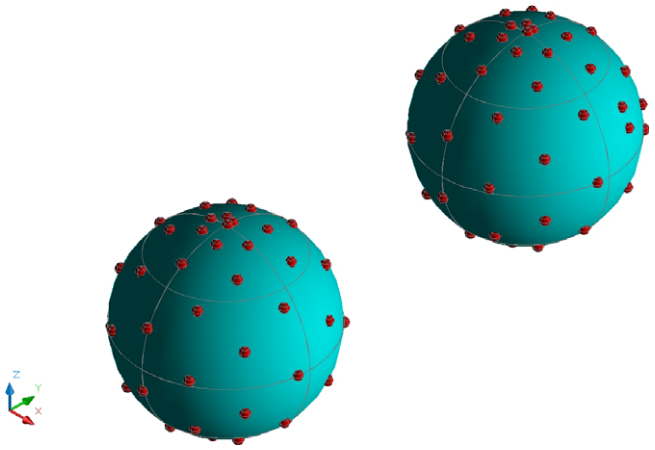

Fig. 8. Distribution of collocation points for two spheres ($M = 10$).

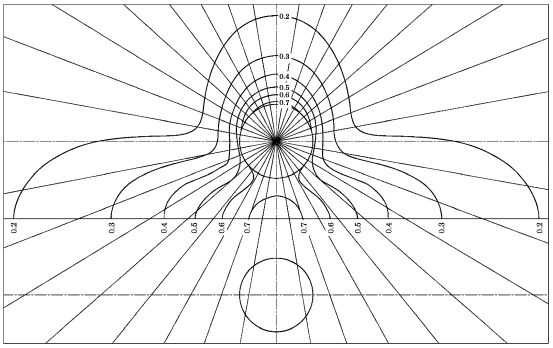

Fig. 9a. Pressure contours by using the SHIE ($z = 0$ and $ka = 1$).

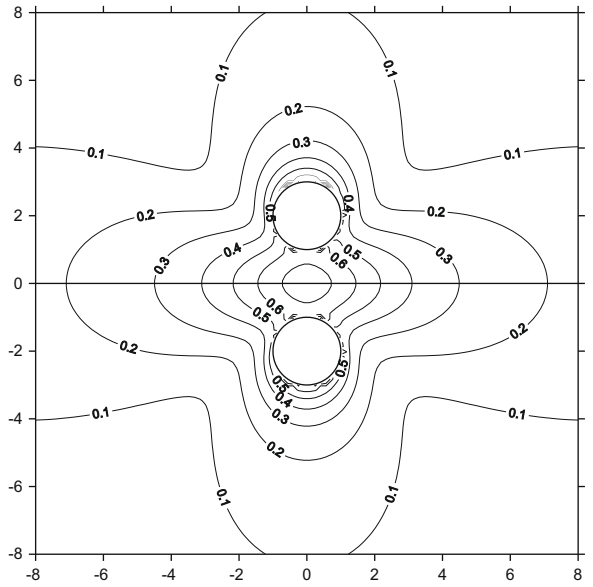

Fig. 9b. Pressure contours by using the present approach ($z = 0$ and $ka = 1$).

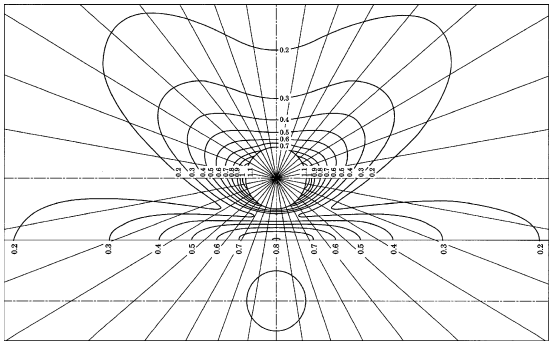

Fig. 10a. Pressure contours by using the SHIE ($z = 0$ and $ka = 2$).

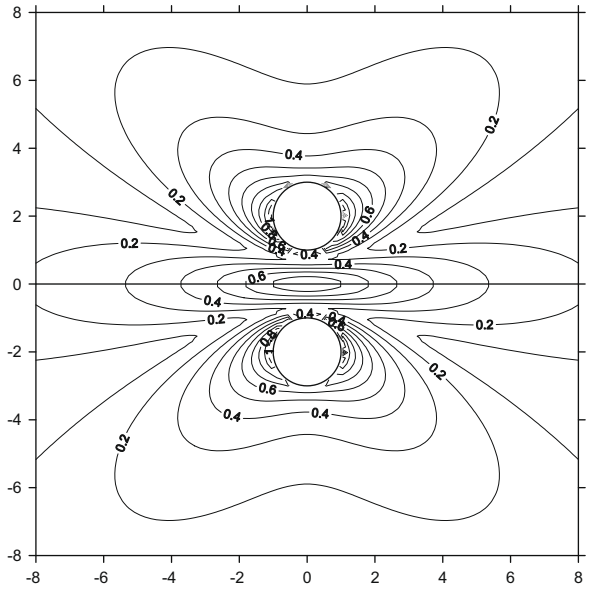

Fig. 10b. Pressure contours by using the present approach ($z = 0$ and $ka = 2$).

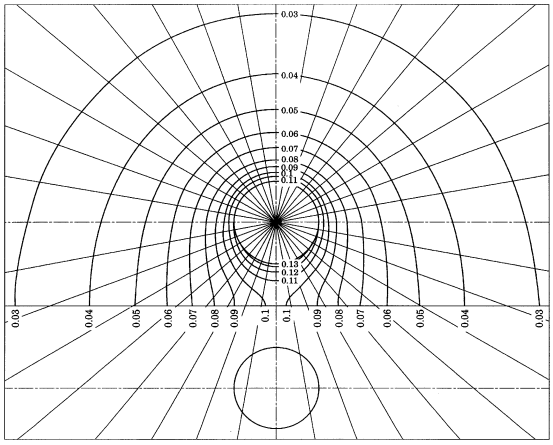

Fig. 11a. Pressure contours by using the SHIE ($z = 0$ and $ka = 0.1$).

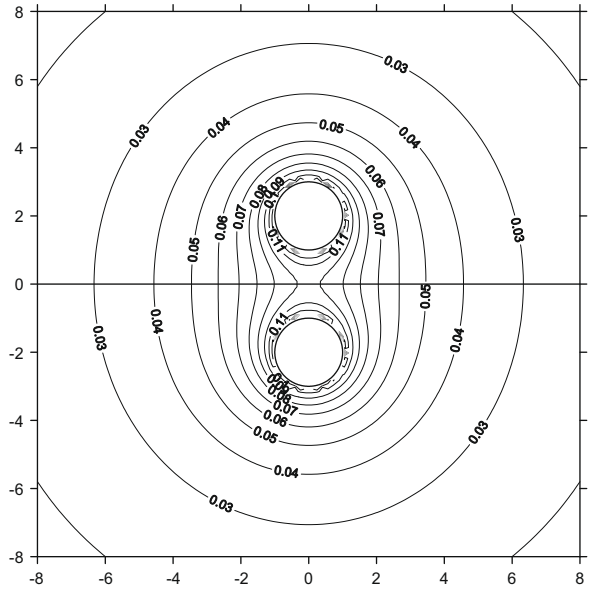

Fig. 11b. Pressure contours by using the present approach ($z = 0$ and $ka = 0.1$).

In the case 1, it is found that the analytical solution for the simple case (one-sphere) can be derived by using our approach. For more than two-spheres case, the boundary density representation is truncated to a finite number of terms. The collocation points are located on the real boundary to match boundary conditions and the unknown spherical harmonics coefficients can be easily determined. Since the error is attributed from the truncated finite number of terms of spherical harmonics coefficients, our approach can be seen as one kind of semi-analytical methods.

Case 3 Acoustic scattering by a sphere

In this case, the scattering problem of a sphere subject to an incident plane wave [23] is considered. Not only hard sphere (Neumann type) but also soft sphere (Dirichlet type) is considered. The plane wave incidence is given as

$$\begin{aligned} u^{inc} &= e^{ik[z\cos\theta_0+\sin\theta_0(x\cos\phi_0+y\sin\phi_0)]} \\ &= \sum_{v=0}^{\infty}(2v+1)i^v\sum_{w=0}^{v}\varepsilon_w\frac{(v-w)!}{(v+w)!}j_v(k\rho)P_v^w(\cos\theta_0)P_v^w(\cos\theta) \\ &\quad\times\cos w(\varphi-\varphi_0), \end{aligned} \tag{55}$$

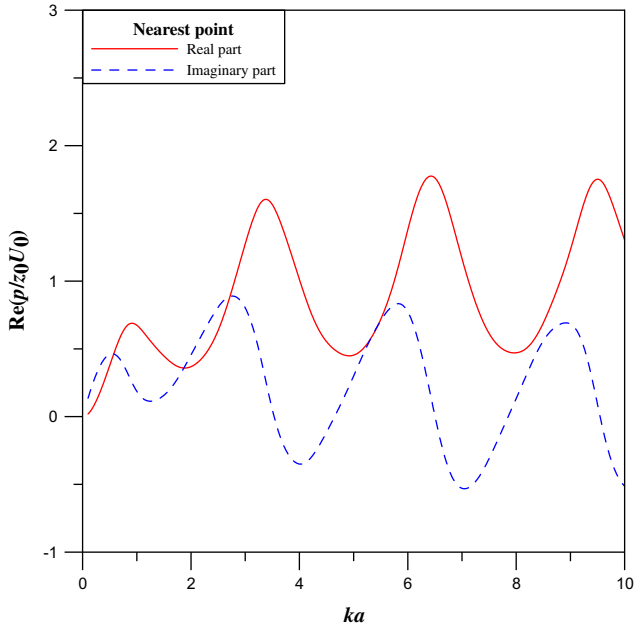

Fig. 12a. The potential on the nearest point versus the wave number ka.

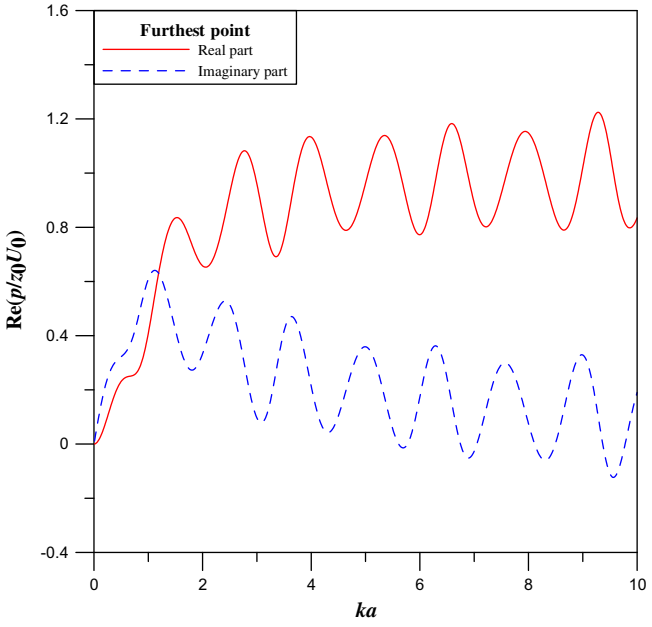

Fig. 12b. The potential on the furthest point versus the wave number ka.

where (θ_0, ϕ_0) defines the angle of the plane wave in the spherical coordinates as shown in Fig. 13. When θ_0 is equal to 0 or π, it denotes the plane wave coming from $+z$ or $-z$ axis, and w is equal to zero. The total potential velocity is superimposed by

$$u = u^{inc} + u^r, \tag{56}$$

where u^r denotes the scattering field and it is solved by using the proposed approach. For the soft sphere $(u = 0)$, we obtain

$$u^r = -u^{inc}, \tag{57}$$

and the spherical coefficients are

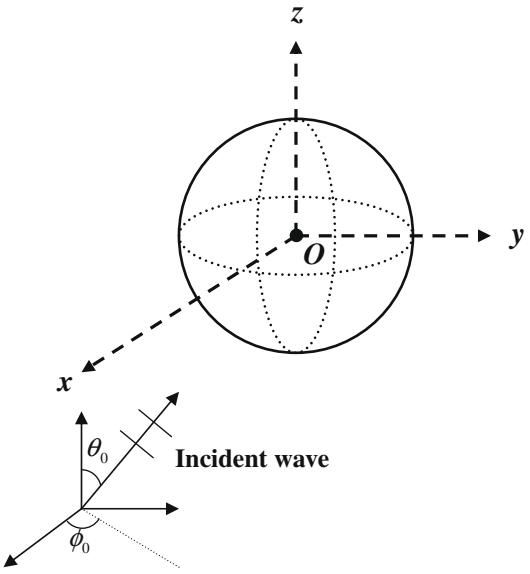

Fig. 13. A scatterer and the incident wave.

$$A_{vw} = -i^v \varepsilon_w (2v+1) \frac{(v-w)!}{(v+w)!} P_v^w(\cos\theta_0) j_v(ka) \cos(w\phi_0), \tag{58}$$

After using the null-field integral equation in Eq. (14), the unknown boundary coefficients are obtained

$$B_{vw} = k i^v \varepsilon_w (2v+1) \frac{(v-w)!}{(v+w)!} P_v^w(\cos\theta_0) j_v(ka) \frac{h_v'^{(2)}(ka)}{h_v^{(2)}(ka)} \times \cos(w\phi_0), \tag{59}$$

Then, the analytical form of the total field is

$$u = \sum_{v=0}^{\infty} \sum_{w=0}^{v} i^v \varepsilon_w (2v+1) \times \frac{(v-w)!}{(v+w)!} \left(j_v(k\rho) + j_v(ka) \frac{h_v^{(2)}(k\rho)}{h_v^{(2)}(ka)} \right) P_v^w(\cos\theta_0) P_v^w(\cos\theta) \times \cos w(\phi - \phi_0). \tag{60}$$

For the same procedure, the hard sphere $(t = 0)$ is considered and the analytical solution is obtained as

$$u = \sum_{v=0}^{\infty} \sum_{w=0}^{v} i^v \varepsilon_w (2v+1) \times \frac{(v-w)!}{(v+w)!} P_v^w(\cos\theta_i) P_v^w(\cos\theta) \left(j_v(k\rho) + j_v'(ka) \frac{h_v^{(2)}(k\rho)}{h_v'^{(2)}(ka)} \right) \cos(w\phi_i) \times \cos(w\phi). \tag{61}$$

For the numerical implementation, M is given 10 and 66 collocation points are needed. Fig. 14a and b show the scattering parameter S versus the polar angle (θ) for $ka = 1$ and 2, respectively, where the scattering parameter S is defined by

$$p^s(\rho) = \frac{e^{-ik\rho}}{k\rho} S(\boldsymbol{\rho} \to \infty). \tag{62}$$

Good agreement is observed after comparing with the result of Chandrasekhar and Rao [23].

Case 4 Acoustic scattering by two spheres

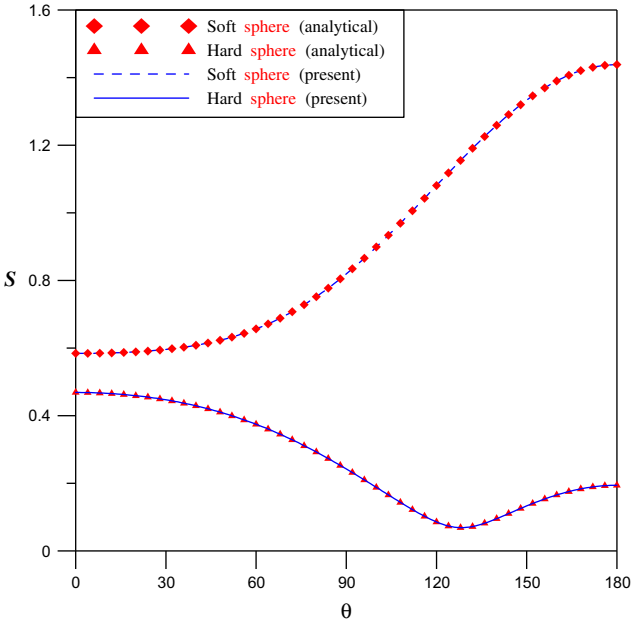

Fig. 14a. Scattering parameter S versus the polar angle θ for $ka = 1$.

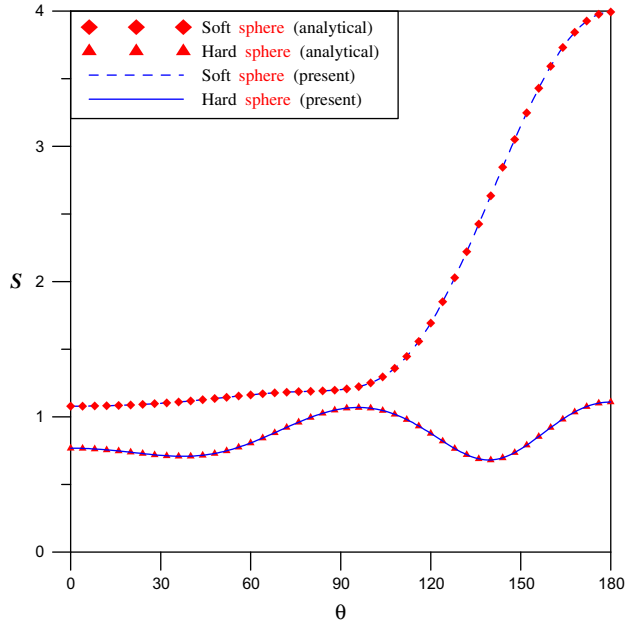

Fig. 14b. Scattering parameter S versus the polar angle θ for $ka = 2$.

After successfully verifying the scattering results of one-sphere, we extend to deal with the two-spheres case subject to an incident wave as shown in Fig. 15. The problem has been solved by Peterson and Ström [11]. By using the null-field integral equation approach, the M number of terms is taken 10 and 66 points are distributed on each sphere. The radar cross section (RCS) is defined in the form

$$\sigma_N(\rho, \theta, \phi; \theta_0, \phi_0) = 4\pi\rho^2 \frac{|u^s|^2}{|u^{inc}|^2} \frac{1}{\pi a^2}. \tag{63}$$

It is noted that the normalized radar cross section is defined as

$$\sigma_N^A(\theta, \phi; \theta_0, \phi_0) = \lim_{\rho \to \infty} \sigma_N(\rho, \theta, \phi; \theta_0, \phi_0), \tag{64}$$

when the observed radius ρ is at infinity. Figs. 16a and 16b show the asymptotic backscattering cross section $\sigma_N^A(\pi/2,\pi;\pi/2,0)$ versus the separation $(2kd)$ for soft and hard spheres, respectively at $ka=2$. Since the real data of Peterson and Ström are not easy to obtain, we used the digitizing skill to reconstruct their solution. Although a little deviation on digitalizing and transforming the data may be present, it can be observed that the results of our approach agree well with those of Peterson and Ström. Fig. 17 shows the asymptotic backscattering cross section $\sigma_N^A(\pi-\theta',\pi;\theta',0)$ for $ka=2$ and $2kd=4.5$ subject to hard and soft boundary conditions. After comparing with the results of Peterson and Ström, good agreement is made. Figs. 18a and 18b show the $\sigma_N(10,\theta,0;\pi/2,0)$ and $\sigma_N^A(\theta,0;\pi/2,0)$ of soft and hard spheres for $ka=2$ and $2kd=4.5$, respectively. It is found that our results match well with those of Peterson and Ström when the distance is located at infinity. However, there also exists some discrepancy for σ_N at other places. We wonder that the deviation stems from the numerical calculation. The accuracy of the digital number of the computer in the early years is lower than that of the present one. At infinity, we can employ the asymptotic formulae of spherical Hankel function. This is the reason why σ_N^A agrees well, but σ_N has little deviation at other places.

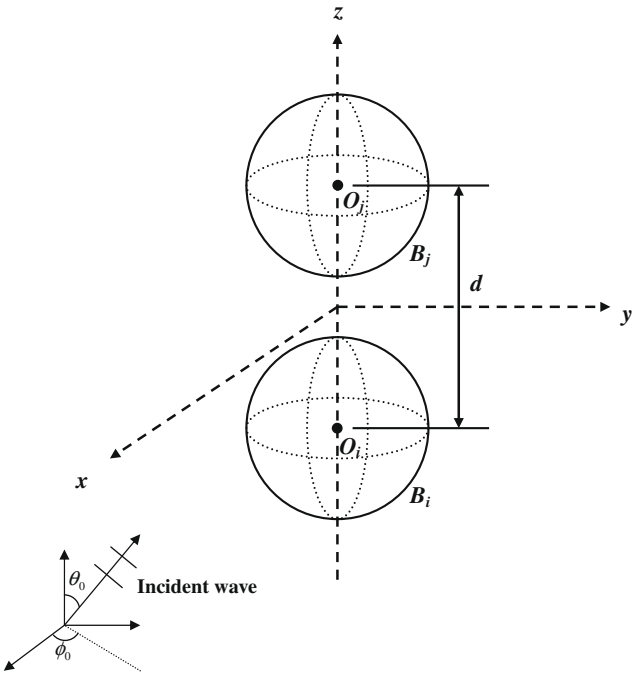

Fig. 15. A scattering problem of two spheres and the incident wave.

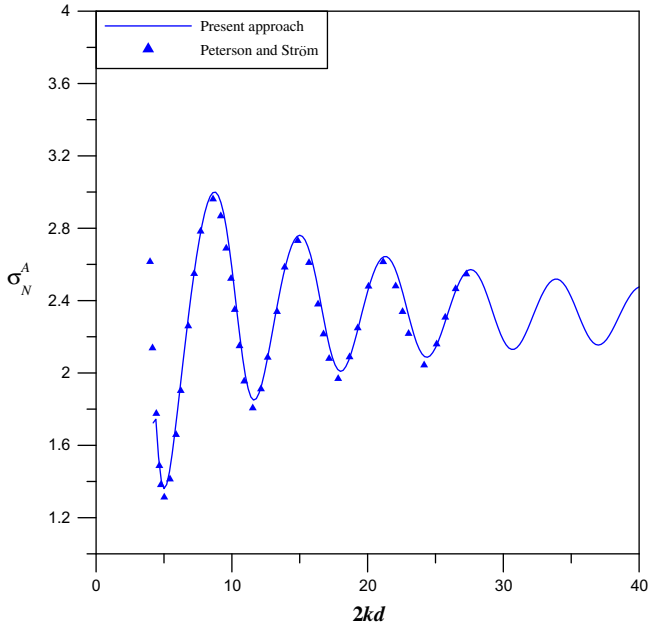

Fig. 16b. Asymptotic backscattering cross section $\sigma_N^A(\pi/2,\pi;\pi/2,0)$ versus the separation $(2kd)$ for the hard spheres $(ka=2)$.

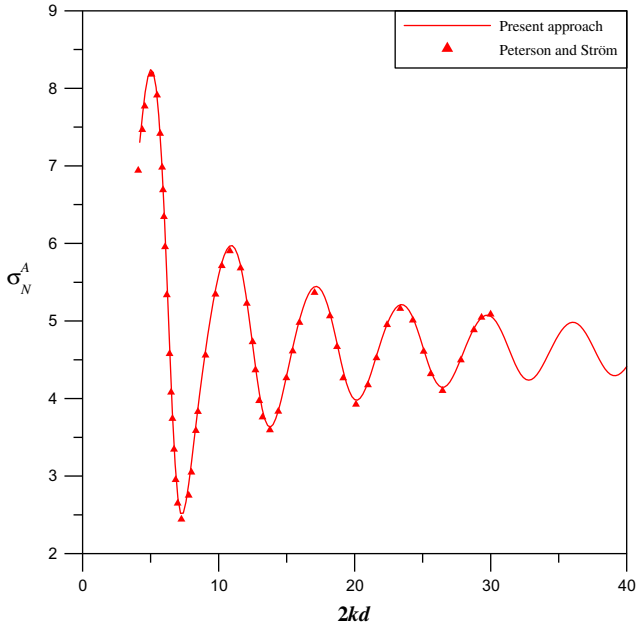

Fig. 16a. Asymptotic backscattering cross section $\sigma_N^A(\pi/2,\pi;\pi/2,0)$ versus the separation $(2kd)$ for the soft spheres $(ka=2)$.

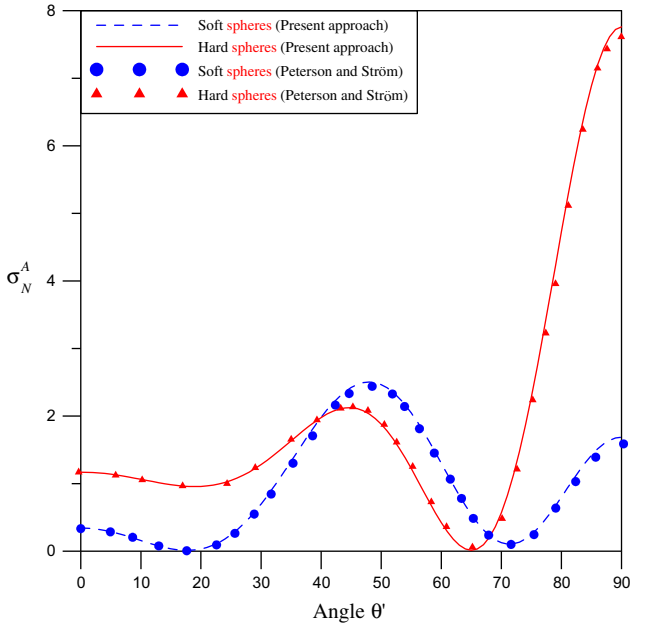

Fig. 17. Asymptotic backscattering cross section $\sigma_N^A(\pi-\theta',\pi;\theta',0)$ for $ka=2$ and $2kd=4.5$ subject to hard and soft boundary conditions.

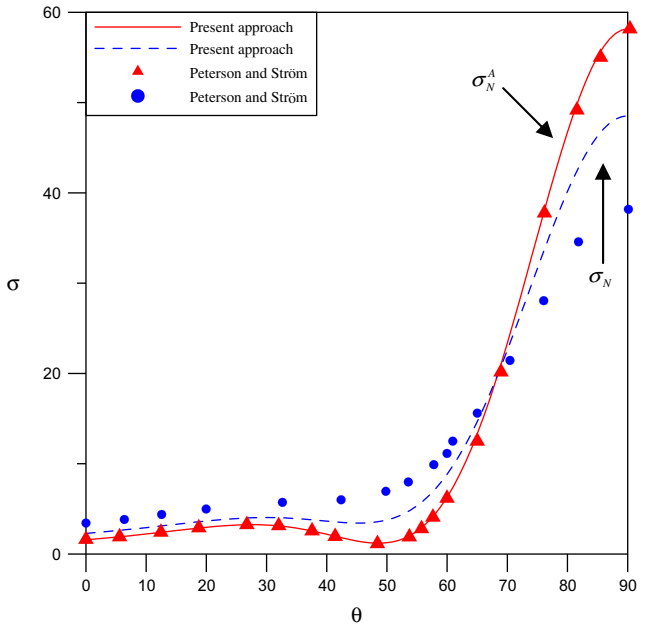

Fig. 18a. The $\sigma_N(10,\theta,0;\pi/2,0)$ and $\sigma_N^A(\theta,0;\pi/2,0)$ of the soft spheres for $ka=2$ and $2kd=4.5$.

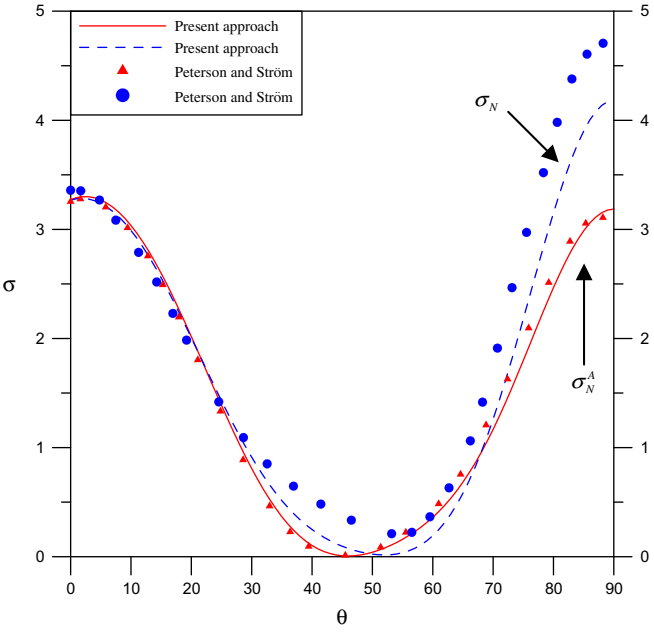

Fig. 18b. $\sigma_N(10,\theta,0;\pi/2,0)$ and $\sigma_N^A(\theta,0;\pi/2,0)$ of the hard spheres for $ka=2$ and $2kd=4.5$.

4. Conclusions

For the three-dimensional radiation and scattering problems with multiple spheres, we have proposed a null-field integral equation formulation by using degenerate kernels and spherical harmonics in companion with adaptive observer systems. This method is a semi-analytical approach for Helmholtz problems with spherical boundaries since only truncation error in the spherical harmonics is involved. Although cases of one and two spheres are used, the present approach can be straightforward extended to solve more general problems with radiators or scatters of arbitrary number, different radii and various positions without any difficulty. In addition, fictitious frequencies can be suppressed by using the Burton and Miller approach. A general-purpose program for solving radiation problem with arbitrary number, different size and various locations of spheres was developed. Pressure contours as well as RCS were compared well with the exact solution and other numerical solutions.

Acknowledgement

This research was partially supported by the National Science Council in Taiwan through Grant NSC97-2221-E-019-015-MY3 and 98-EC-17-A-05-S2-0143 from the Ministry of Economic Affairs of R.O.C.

References

[1] Burton AJ, Miller GF. The application of integral equation methods to numerical solution of some exterior boundary value problems. Proc Roy Soc Ser A 1971;323:201–10.
[2] Schenck HA. Improved integral formulation for acoustic radiation problem. J Acous Soc Am 1968;44:41–58.
[3] Chen JT, Chen KH, Chen IL, Liu LW. A new concept of modal participation factor for numerical instability in the dual BEM for exterior acoustics. Mech Res Commun 2003;26(2):161–74.
[4] Seybert AF, Rengarajan TK. The use of CHIEF to obtain unique solutions for acoustic radiation using boundary integral equations. J Acous Soc Am 1968;81:1299–306.
[5] Wu TW, Seybert AF. A weighted residual formulation for the CHIEF method in acoustics. J Acoust Soc Am 1991;90(3):1608–14.
[6] Lee L, Wu TW. An enhanced CHIEF method for steady-state elastodynamics. Eng Anal Bound Elem 1993;12:75–83.
[7] Ohmatsu S. A new simple method to eliminate the irregular frequencies in the theory of water wave radiation problems. Papers of Ship Research Institute 70; 1983.
[8] Chen IL. Using the method of fundamental solutions in conjunction with the degenerate kernel in cylindrical acoustic problems. J Chin Inst Eng 2006;29(3):445–57.
[9] Dokumaci E, Sarigül AS. Analysis of the near field acoustic radiation characteristics of two radially vibrating spheres by the Helmholtz integral equation formulation and a critical study of the efficacy of the CHIEF over determination method in two-body problems. J Sound Vib 1995;187(5):781–98.
[10] Waterman PC. New formulation of acoustic scattering. J Acoust Soc Am 1969;45(6):1417–29.
[11] Peterson B, Ström S. Matrix formulation of acoustic scattering from an arbitrary number of scatterers. J Acoust Soc Am 1974;56(3):771–80.
[12] Liang C, Lo YT. Scattering by two spheres. Radio Sci 1967;2(12):1481–95.
[13] Gaunaurd GC, Huang H. Acoustic scattering by a pair of spheres. J Acoust Soc Am 1995;98(1):495–507.
[14] Rao SM, Raju PK. Application of the method of moments to acoustic scattering from multiple bodies of arbitrary shape. J Acoust Soc Am 1989;86(3):1143–8.
[15] Chen JT, Shen WC, Chen PY. Analysis of circular torsion bar with circular hole using null-field approach. Comp Model Eng Sci 2006;12(2):109–19.
[16] Chen JT, Lee YT, Lin YJ. Interaction of water waves with an array of vertical cylinders using null-field integral equations. Appl Ocea Res 2009;31:101–10.
[17] Chen JT, Hsiao CC, Leu SY. A new method for Stokes' flow with circular boundaries using degenerate kernel and Fourier series. Int J Numer Meth Eng 2008;74:1955–87.
[18] Lee WM, Chen JT. Null-field integral equation approach for free vibration analysis of circular plates with multiple circular holes. Comput Mech 2008;42:733–47.
[19] Chen JT, Wu AC. Null-field approach for piezoelectricity problems with arbitrary circular inclusions. Eng Anal Boun Elem 2006;30:971–93.
[20] Chen JT, Lee YT, Lee WM. A semi-analytical approach for boundary value problems with circular boundaries. In: Manolis GD, Polyzos D, editors. Recent advances in boundary methods: a volume to Honor Professor Dimitri Beskos, Springer-Verlag; 2009.
[21] Seybert AF, Soenarko B, Rizzo FJ, Shippy DJ. An advanced computational method for radiation and scattering of acoustic waves in three dimensions. J Acoust Soc Am 1985;77(2):362–8.
[22] Abramowitz M, Stegun IA. Handbook of mathematical functions with formulas, graphs, and mathematical tables. New York: Dover; 1965.
[23] Chandrasekhar B, Rao SM. Elimination of internal resonance problem associated with acoustic scattering by three-dimensional rigid body. J Acoust Soc Am 2004;115(6):2731–7.